

## Local Dose Distribution in Cell Nucleus from Gold Nanoparticles with Radioisotopes

Taewan Kim<sup>a</sup>, Changmin Lee<sup>a</sup>, Yoonho Na<sup>a</sup>, Kyuri Kim<sup>a</sup>, Sung-Joon Ye<sup>a,b,c,d\*</sup>

<sup>a</sup>Department of Applied Bioengineering, Graduate School of Convergence Science and Technology, Seoul National University, Seoul, 08826, Republic of Korea

<sup>b</sup>Research Institute for Convergence Science, Seoul National University, Seoul, 08826, Republic of Korea

<sup>c</sup>Advanced Institute of Convergence Technology, Seoul National University, Suwon, 16229, Republic of Korea

<sup>d</sup>Biomedical Research Institute, Seoul National University Hospital, Seoul, 03080, Republic of Korea

\*Corresponding author: sye@snu.ac.kr

**\*Keywords :** Gold Nanoparticle, Radionuclide Therapy, Local Dose Distribution

### 1. Introduction

Gold nanoparticles (GNP) have emerged as promising radiosensitizers due to their unique properties facilitating tumor cell permeation and exerting cytotoxic effects. [1] Combining GNP with radioisotopes (RI) has garnered considerable interest in both therapeutic and imaging applications. [2] This combination exploits the enhanced permeability and retention (EPR) effect, leading to improved RI accumulation and prolonged retention within tumor tissues.

While numerous studies have focused on calculating radiation doses from nuclear medicine, their relevance to therapeutic response remains uncertain, precluding their integration into standard clinical practice. [3] However, recognizing the significance of microscopic dose distribution, some researchers have explored its implications, particularly in radionuclide therapy.

The local distribution of RI within the tumor microenvironment significantly influences microscopic dose distribution, primarily due to the short range of emitted charged particles. Previous investigations have demonstrated that the intracellular distribution of RI profoundly impacts the outcomes of in vitro experiments involving metal nanoparticles with Auger electron emitters.

In this context, our study aims to elucidate the absorbed nucleus dose and its local distribution from GNP combined with three different RIs (<sup>103</sup>Pd, <sup>125</sup>I, and <sup>177</sup>Lu). By obtaining radial dose distributions from GNP with RIs, we can calculate the nucleus dose and assess its local distribution.

### 2. Methods and Results

In this part, the methods for investigating nucleus dose and intranuclear dose distribution and the results from them are illustrated. Monte Carlo simulation and convolution method with C++ were used in this study.

#### 2.1 Radial dose distribution

Using Monte Carlo simulation with Geant4, we obtained radial dose distributions from GNP labeled with RI. Assuming the cell material as liquid water, we calculated absorbed doses within a 5 mm-radius water sphere surrounding the GNP. The simulations considered a 50 nm spherical GNP and included physics models for Geant4\_DNA\_AU in gold and Geant4\_DNA in water, tracking electron transport down to 100 eV. Auger effect, Auger cascade, PIXE, and atomic relaxation processes were activated. Three radioisotopes, including two auger electron emitters (<sup>103</sup>Pd, <sup>125</sup>I) and one beta emitter (<sup>177</sup>Lu), were considered for calculation. Results showed that <sup>125</sup>I had the highest absorbed dose below 600 nm, followed by <sup>103</sup>Pd, which rapidly decreased due to the short electron range. Despite low dose values of <sup>177</sup>Lu, its long-range beta electrons could impact regions beyond 1 mm.

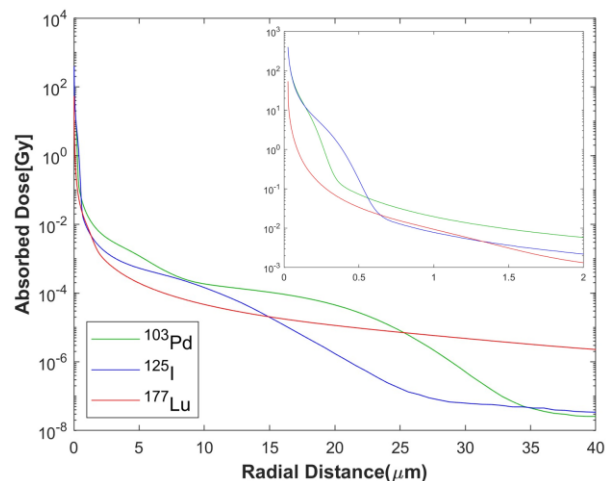


Fig. 1. Radial dose distribution from GNP with 3 RIs. (same data at the vicinity region is inserted.)

#### 2.2 Nucleus dose

In this study, we focused on calculating nucleus doses within MDA-MB-231 human breast cancer cells. Adopting a cylindrical cell geometry with dimensions derived from a previous study [4], the cell had a

diameter of 13.5  $\mu\text{m}$ , with a nucleus diameter of 8  $\mu\text{m}$ , and an extracellular matrix (ECM) covering the cell with a thickness of 2.5  $\mu\text{m}$ . Two distributions of gold nanoparticles (GNP) were considered: GNP within the cytoplasm and the ECM. Both uniform and random distributions of GNP were investigated to assess the impact of distribution heterogeneity.

Using C++ and voxel-based convolution techniques, we calculated the nucleus dose based on the radial dose distribution obtained from Geant4 simulations. Assuming an activity of 500  $\mu\text{Bq}$  for each radioisotope labeled with a single GNP, we considered the half-life of each radioisotope when calculating the time-integrated activity (TIA) for nucleus dose determination.

Results showed that nucleus doses from  $^{103}\text{Pd}$  exhibited the highest values, while those from  $^{177}\text{Lu}$  showed the lowest. Notably, variations in results were significant when GNPs were distributed in the cytoplasm, particularly between random and uniform distributions. However, only the results for  $^{125}\text{I}$  with GNP distribution in the cytoplasm showed significant differences between uniform and random distributions.

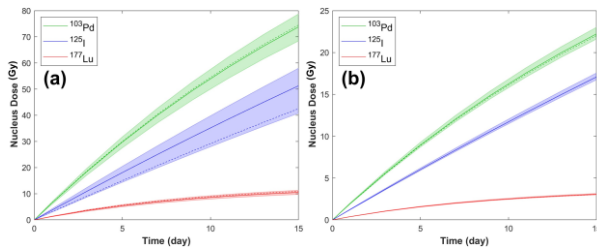


Fig. 2. Nucleus dose as a function of time after injection with GNP distribution in (a) cytoplasm and (b) ECM.

Dose rates at each time point decreased due to radioisotope decay, with the rate of decrease inversely proportional to the half-life of each radioisotope, resulting in  $^{125}\text{I}$  exhibiting the slowest rate of decrease.

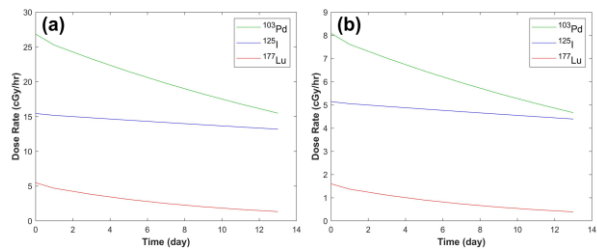


Fig. 3. Dose rate for nucleus with GNP distribution in (a) cytoplasm and (b) ECM.

### 2.3 Intranuclear dose distribution

Using C++, we obtained local dose distributions at  $10 \times 10 \times 10 \text{ nm}^3$  voxels, focusing on the mid-height (1000 nm) of the cylindrical cell. The positions of gold nanoparticles (GNP) were visualized using a gray colormap, with darker shades representing proximity to a visualized slice of the nucleus.

Significant heterogeneity was observed in the local dose distribution when RI-labeled GNPs were located in the cytoplasm. Particularly with  $^{125}\text{I}$ , the nucleus area near the sources exhibited extremely high doses, primarily influenced by low-energy electrons ( $< 5 \text{ keV}$ ). Similar trends were observed with  $^{103}\text{Pd}$ , although the dose distribution with  $^{177}\text{Lu}$  showed less heterogeneity.

Intranuclear doses with GNPs in the ECM demonstrated much lower values compared to those with GNPs in the cytoplasm. Notably, higher doses were observed at the edge of the nucleus in these results. In this scenario, electrons with energy over 20 keV had a significant impact.

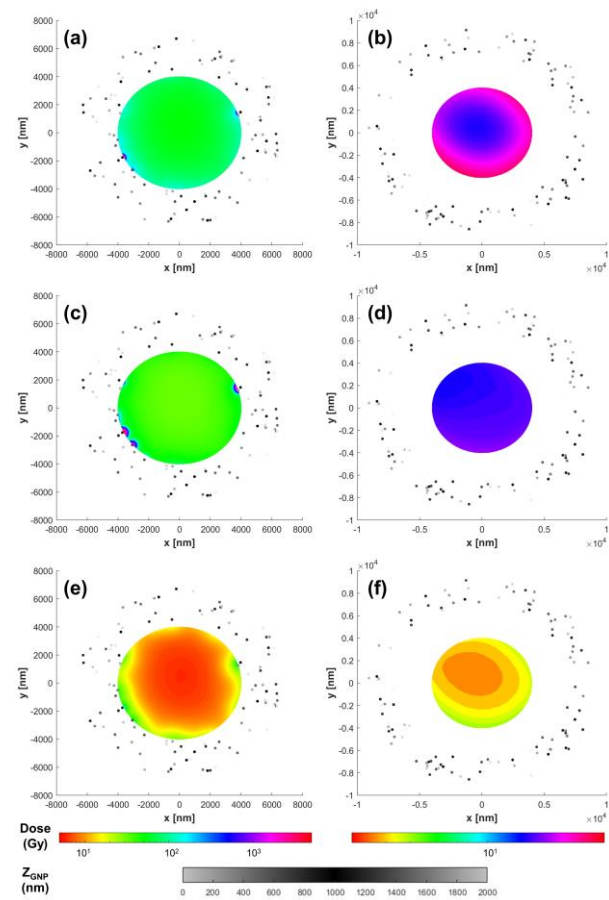


Fig. 4. Visualized local dose distribution in cell nuclear from GNP with (a)  $^{103}\text{Pd}$ , (c)  $^{125}\text{I}$ , and (e)  $^{177}\text{Lu}$  in the cytoplasm and that from GNP with (b)  $^{103}\text{Pd}$ , (d)  $^{125}\text{I}$ , and (f)  $^{177}\text{Lu}$  in the ECM.

### 3. Conclusions

Our study provides several insights into the nuclear dose and its local distribution from GNP labeled with RI. Through Monte Carlo simulations with Geant4, we elucidated the radial dose distribution surrounding GNPs, considering the properties of three different RIs:  $^{103}\text{Pd}$ ,  $^{125}\text{I}$ , and  $^{177}\text{Lu}$ . Our findings underscored the importance of understanding microscopic dose

distribution, particularly within the nucleus, for optimizing radionuclide therapy outcomes.

Calculation of nucleus doses within MDA-MB-231 human breast cancer cells revealed significant variations among the different radioisotopes, with  $^{103}\text{Pd}$  exhibiting the highest values and  $^{177}\text{Lu}$  showing the lowest. The distribution of GNPs within the cytoplasm versus the ECM also significantly impacted the local dose distribution, with heterogeneous dose profiles observed, especially with  $^{125}\text{I}$ . These results emphasize the need to carefully consider the spatial distribution of GNPs and RIs within cancer cells to maximize therapeutic efficacy while minimizing normal tissue toxicity.

Furthermore, our study highlighted the potential of low-energy electrons ( $< 5$  keV) from  $^{125}\text{I}$  to induce extremely high doses within the nucleus, particularly when GNPs were located in the cytoplasm. Conversely, higher energy electrons ( $> 20$  keV) had a significant impact on intranuclear dose distribution when GNPs were in the ECM.

These insights provide valuable guidance for optimizing the design and delivery of nanoparticle-based radiotherapeutics for cancer treatment. Several experimental studies have yielded diverse results in nanoparticle-based radionuclide therapy, even when employing the same RI and nanoparticle. [5] Researchers have speculated that these discrepancies may stem from variations in the distribution of radiation sources; however, a clear elucidation of this phenomenon has remained elusive. With the findings from our study, we provide a clearer explanation for this phenomenon, uncovering the impact of nanoparticle localization and local dose distribution within cancer cells.

Moving forward, further research is warranted to validate our computational simulations and explore additional factors that may influence dose distribution, such as cellular uptake mechanisms and surface functionalization. Additionally, experimental validation of our findings using advanced imaging techniques could provide complementary insights and enhance the translational potential of nanoparticle-based radiotherapeutics in clinical settings. Using the data in this study, we can develop a model for predicting biological effectiveness, especially considering local dose distribution like local effect model (LEM) or microdosimetric kinetic model (MKM), which are already developed for ion therapy.

In summary, our study contributes to advancing the field of radionuclide therapy by providing a comprehensive understanding of the dose distribution within cancer cells treated with RI-labeled GNP. By optimizing the spatial distribution of radiation doses, we can improve the effectiveness and safety of nanoparticle-mediated radiotherapy, ultimately leading to better outcomes for patients.

#### **4. Acknowledgements**

This work was supported by the National Research Foundation of Korea (NRF) grant funded by the Korea government (MSIT) (No. RS-2023-00237149).

#### **REFERENCES**

- [1] Xu, L., Xu, M., Sun, X., Feliu, N., Feng, L., Parak, W. J., & Liu, S., Quantitative comparison of gold nanoparticle delivery via the enhanced permeation and retention (EPR) effect and mesenchymal stem cell (MSC)-based targeting. *ACS nano*, 17(3), 2039-2052, 2023.
- [2] Daems, N., Michiels, C., Lucas, S., Baatout, S., & Aerts, A., Gold nanoparticles meet medical radionuclides. *Nuclear Medicine and Biology*, 100, 61-90, 2021.
- [3] Lawhn-Heath, C., Hope, T. A., Martinez, J., Fung, E. K., Shin, J., Seo, Y., & Flavell, R. R., Dosimetry in radionuclide therapy: the clinical role of measuring radiation dose. *The lancet oncology*, 23(2), e75-e87., 2022.
- [4] Sung, W., Ye, S. J., McNamara, A. L., McMahan, S. J., Hainfeld, J., Shin, J., et al., Dependence of gold nanoparticle radiosensitization on cell geometry. *Nanoscale*, 9(18), 5843-5853, 2017.
- [5] Wawrowicz, K., Żelechowska-Matysiak, K., Majkowska-Pilip, A., Wierzbicki, M., & Bilewicz, A., Platinum nanoparticles labelled with iodine-125 for combined “chemo-Auger electron” therapy of hepatocellular carcinoma. *Nanoscale Advances*, 2023.